3.5 Beam Physics

3.5.1 Ion Trapping

The electron beam circulating in the storage ring ionizes the molecules of the residual gas. Ions within the beam region in turn experience the time dependent Coulomb field of the electron beam and under certain conditions can be accumulated in the bunch existing region. These lead to increasing of the local gas pressure within the beam volume and reduce therefore the beam lifetime.

The ion trapping into the bunch is caused by the stable (periodical) motion of ions around the bunch trajectory driven by the Coulomb field of the electron bunches. The probability of the ions stable motion increases with the high degree of periodicity of the beam charge distribution in the storage ring. In the limiting case, when all the RF buckets of the ring are filled by the electron bunches (in case of CANDLE 360 bunches), the restoring force experienced by the residual gas ions is exactly periodic in time. The ions experience drift at the interval between bunch spacing and get a "kick" when the subsequent bunch arrives a position of the ion location.

In linear approximation, in the case of periodical distribution of the bunches in the storage ring (the harmonic number h is equal to the number of circulating bunches h_b), the result of the combination of ion single kick and drift can be written in the matrix form:

$$\begin{pmatrix} u \\ \dot{u} \end{pmatrix} = M_u \begin{pmatrix} u_0 \\ \dot{u}_0 \end{pmatrix}, \; M_u = \begin{pmatrix} 1 & t_b \\ 0 & 1 \end{pmatrix} \begin{pmatrix} 1 & 0 \\ -a_u & 1 \end{pmatrix} \tag{3.5.1}$$

where $u = x, y$ are the horizontal and vertical ion coordinates respectively, $\dot{u}$ is the ion transverse velocity, t_b is the time between the passages of successive electron bunches, a_u is the ion kick factor. The ion kick factor is caused by the circulating electron beam Coulomb field and is given by

$$a_{x,y} = -\frac{2N_b r_p c}{A\sigma_{x,y}\left(\sigma_x + \sigma_y\right)} \tag{3.5.2}$$

with r_p the classical proton radius, N_b the number of the particles in the electron bunch, $\sigma_{x,y}$ the bunch horizontal and vertical transverse sizes and A the ion mass number in units of proton mass. The critical ion masses that define the stability of ion motion in horizontal or vertical planes are given by the stability condition $\left|Tr\left(M_{x,y}\right)\right| = 2$ that in terms of the beam parameters read as

$$A_{crit} = \frac{N_b r_p C}{2b\sigma_{x,y}\left(\sigma_x + \sigma_y\right)} \tag{3.5.3}$$

The ion motion is unstable at a given point of lattice (or the bunch trajectory) when $A < A_{crit} = \max\left(A_{c;x}, A_{c;y}\right)$. The ions are not trapped (are unstable) when the above condition is satisfied for any position along the lattice.

An exact periodic driving force is observed for both single bunch ($h_b = 1$) and filled RF buckets ($h_b = h = 360$) mode of the storage ring operation. For a bunch charge of

$Q = 0.7nC$, single bunch operation drives the trapping of the ions with mass number larger than $A_{crit} = 71.8$. Thus, no ion trapping difficulties are expected for the single-bunch mode operation of the storage ring. If all the RF buckets are filled ($Q = 0.7nC$, current 350 mA), the critical number for the ion mass is $A_{crit} = 0.2$ and all ions are stable and trapped within the bunch volume.

By introducing a gap in the multi-bunch operation mode, the periodicity of the beam charge (driving force) vanishes, thus providing for further drift of the ions until their transverse motion under certain conditions becomes unstable. The modified matrix M for this mode is given by [1,2]:

$$M_{x,y} = \left\{ \begin{pmatrix} 1 & t_b \\ 0 & 1 \end{pmatrix} \begin{pmatrix} 1 & 0 \\ -a_{x,y} & 1 \end{pmatrix} \right\}^{h} \begin{pmatrix} 1 & t_b \\ 0 & 1 \end{pmatrix}^{h-h_b} \tag{3.5.4}$$

The stability condition (stable ion mass) is again given by $|Tr\, M| = 2$. Ions trapped in the CANDLE storage ring have been examined for the range of ion masses $1 \le A \le 50$ for the any possible multi-bunch regime of machine operation. The stability of the transverse motion of the ions has been checked along the regular lattice and the results are presented on the Fig. 3.5.1. The vertical axe indicates the ions mass number with unstable states. The horizontal axe presents the number of the subsequently circulating bunches in the ring. The effect of the ion trapping is observed when the number of bunches in the ring exceeds 90. The optimal value of the number of bunches for the CANDLE storage ring has been defined $h_b = 282$ which provides an ion-cleaning gap of 78 RF buckets not filled with the electrons. With such a cleaning gap, only 6 ions number are stable or trapped.

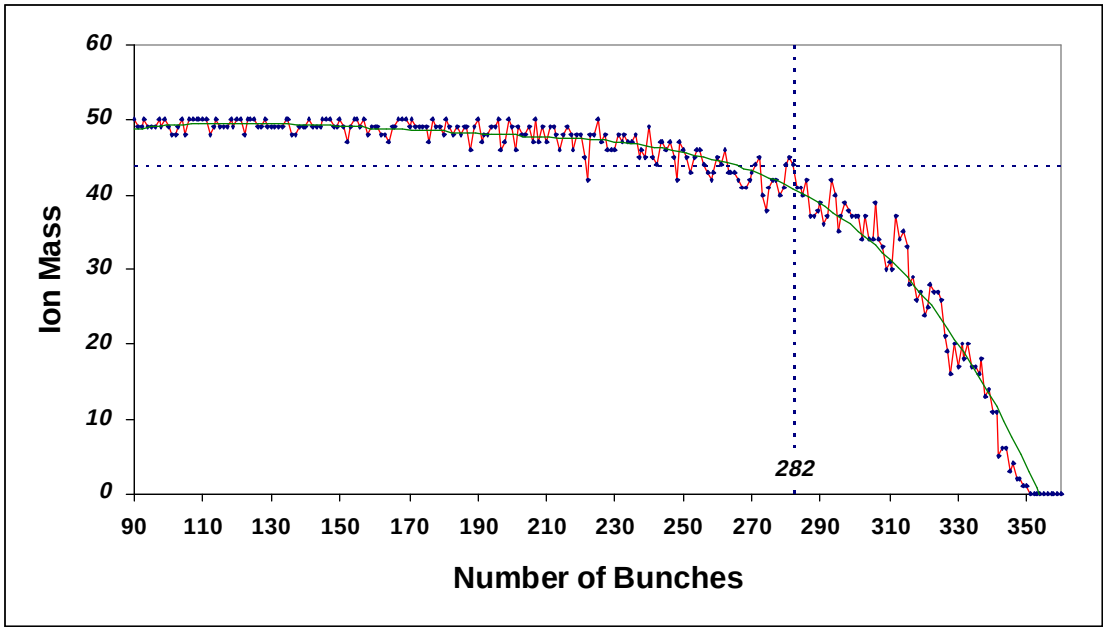

Fig. 3.5.1 Number of unstable ion masses versus number of the circulating bunches in the CANDLE storage ring.

An additional criterion for the optimization of the number of bunches in multi-bunch operation mode is an analysis and comparison of the list of trapped ions with the mass numbers of real residual gas species. Fig. 3.5.2 presents the trapped ion masses versus filled RF buckets.

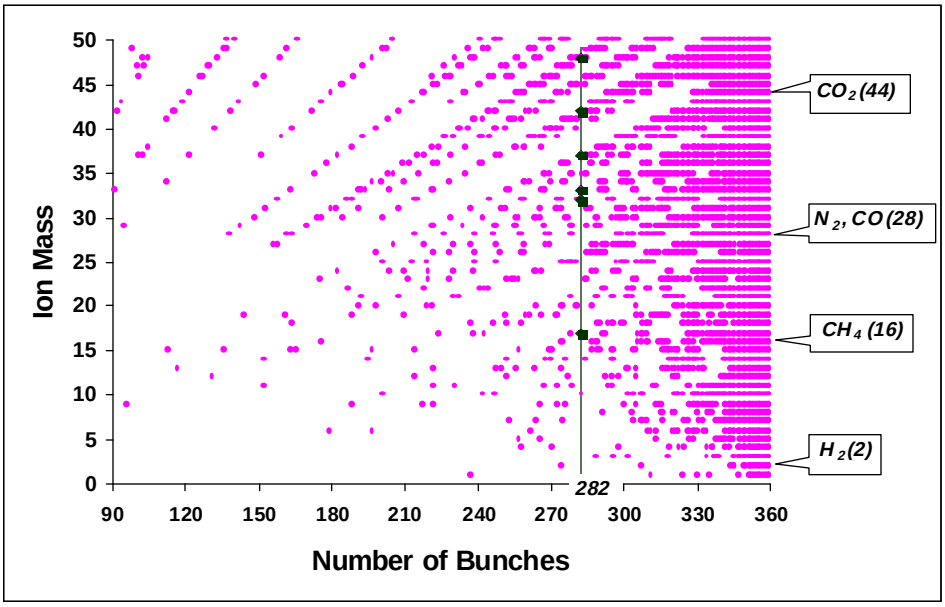

Fig. 3.5.2 The trapped ion masses versus number of the filled RF buckets.

The stable ion mass numbers in CANDLE storage ring are given in Table 3.5.1; the number of bunches is $h_b = 282$. The comparison with species of the ions in the residual gas that can occur in the chamber shows that for the given number of bunches $h_b = 282$ no components of residual gas will lead to trapped ions in the ring.

Table.3.5.1 The trapped ion masses and real residual gas components for 282 bunch operation

Predicted stable ion mass	Residual gas species (masses, species)
-	2, H_2
-	16, CH_4
17	-
-	28 , N_2,CO
32	-
33	-
37	-
42	-
-	44, CO_2
48	-

The chosen number of bunches in the storage ring, 282 bunches from available 360 RF buckets, provides practically trapped ions-free operation of the machine at almost 80% filling.

3.5.2 Single Bunch Instabilities.

The high brightness of the electron beam requires a large circulating current in the ring. The circulating beam interacts with the surrounding vacuum chamber and excites the wakefields due to chamber walls finite conductivity, surface roughness and the geometrical changes in the chamber geometry. In addition, by interacting with the RF cavities, the

beam excites the high order longitudinal and transverse modes that can resonantly affect the beam. These fields that have longitudinal and transverse components act back on the trailing particles (bunches) resulting in particle longitudinal oscillations, effective transverse emittance growth and consequently in the instabilities development depending on the beam current. In the frequency domain, the induced instabilities grow exponentially when the imaginary part of the complex frequency shift $\Delta\Omega_n$ of particular beam oscillation mode, is negative ($\mathrm{Im}\,\Delta\Omega_n < 0$). Fortunately, in electron storage rings the synchrotron radiation provides a natural damping to individual particle oscillations (to any collective bunch motion) that define the instability threshold current I_{thres} given by the condition

$$|\,\mathrm{Im}[\Delta\Omega_n(I)]| < 1/\tau_r \tag{3.5.5}$$

where τ_r is the radiation damping time, i.e. the synchrotron oscillations damping time for longitudinal instabilities or the horizontal, vertical damping times in the transverse case.
The wake fields that act back on the particles of the beam can be divided into two categories short and long-range. The short range wakefields are dominated by the low frequency part of the impedance (broad band impedance) and act basically within the single bunch, i.e. the fields induced by the heading particles act back on the trailing particle of the bunch. As usual, these fields are decay very quickly in time less that one turn, and drive single bunch current dependent instabilities.
The most notable single bunch instability, so-called microwave instability, occurs in the longitudinal plane. The excited longitudinal wake fields induce an extra voltage within the bunch increasing the energy spread that results in the bunch lengthening. The instability is fast and it occurs before the head and tail particles can interchange via the synchrotron oscillations that damp the longitudinal particle oscillations. The threshold current of the microwave instability is given by [3-6]

$$I^{\parallel}_{threshold} = \frac{\sqrt{2\pi}\alpha\sigma_z(E/e)}{R\left|Z_{\parallel}/n\right|_{bb}}\left(\frac{\sigma_\varepsilon}{E}\right)^2 \tag{3.5.6}$$

where E is the particle synchronous energy, e is the electron charge, $\left|Z_{\parallel}/n\right|_{bb}$ is the normalized longitudinal broadband impedance, n is the harmonic number, α is the momentum compaction factor, σ_z is the bunch length, σ_ε/E is the relative energy spread, and R is the average ring radius. The current $I^{\parallel}_{threshold}$ is the average circulating beam current per bunch.
Table 3.5.2 presents the contributions to broadband longitudinal and transverse impedance caused by chamber walls finite conductivity, surface roughness, transitions, BPMs and bellows.

Table 3.5.2 CANDLE Broadband impedance.

	$(Z/n)^{\parallel}_{bb}\ [m\Omega]$		$Z^{\perp}_{bb}\ [k\Omega/m]$	
	Re	Im	Re	Im
Resistive walls	38	38	0.026	0.027
Wall roughness	-	63	3.63	-
Transitions	-	11	-	0.465
BPM's	0.065	0.038	0.32	0.19
Bellows	48	190	6.9	5.5
Total	86	302	10.9	6.2

The normalized machine longitudinal broadband impedance for the CANDLE storage ring is equal to $(Z/n)^{\|}_{bb} = 0.314\Omega$ and is far below the requirement to the Third Generation machine impedance value of $|Z/n|^{\|}_{bb} \sim 1\Omega$. The corresponding single bunch threshold current value is $I^{\|}_{threshold} = 8.9mA$. Note that CANDLE nominal operation current of 350mA implies the single bunch charge of 0.9 nC that corresponds to circulating current of $I = 1.24mA$. Fig. 3.5.3 shows the CANDLE threshold current versus the longitudinal impedance of the storage ring. The single bunch current is below the longitudinal microwave instability threshold current for the less than 2Ω low-frequency broadband impedance of the ring.

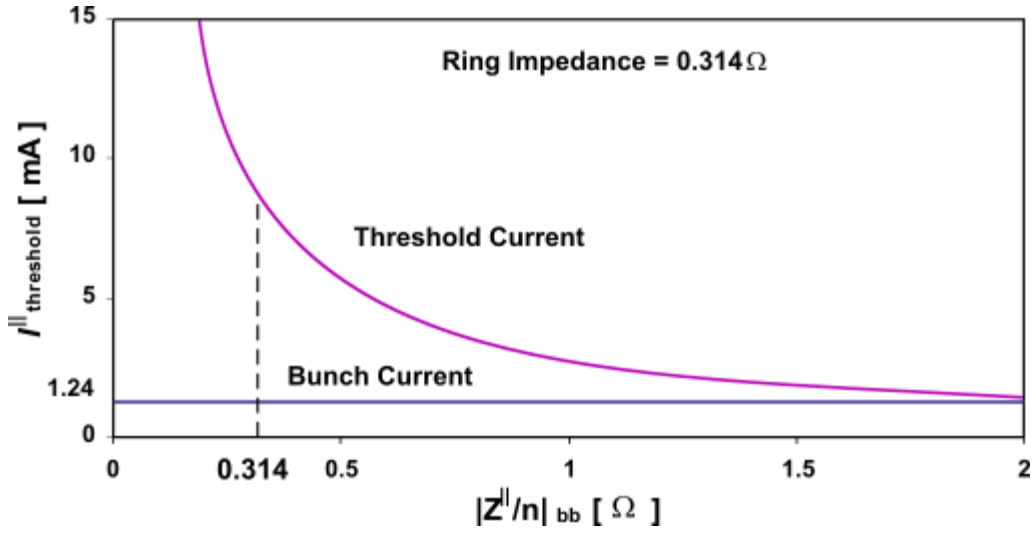

Fig.3.5.3. Longitudinal threshold current versus longitudinal broadband impedance

The transverse wake fields excited by off-axis bunch in the storage ring cause the transverse fast single bunch instability. The wakefields that are excited by the head part of the bunch deflect the tail particles from the center of the chamber thus leading to bunch break-up. The vertical dipole mode is usually dominant in the storage ring as the vertical aperture of the chamber is smaller than the horizontal one. The transverse emittance of the bunch is enlarged until the head and tail particles interchange the longitudinal positions due to synchrotron oscillations. The threshold current of the transverse single bunch instability is given by [2, 6]

$$I^{\perp}_{threshold} = \frac{\sqrt{2\pi}\alpha(E/e)}{\overline{\beta}|Z_{\perp}|_{bb}}\left(\frac{\sigma_{\varepsilon}}{E}\right) \qquad (3.5.7)$$

with $\overline{\beta}$ vertical average beta function ($\overline{\beta}$=10.5m). The threshold current for CANDLE storage ring that defines the process stabilization limit for the transverse single bunch instability is then equal to $I^{\perp}_{threshold} = 113mA$.

The above estimations are conservative: as it follows from Table 3.5.2, the bellows give the most essential inclusion in the threshold currents values, whereas the shielded bellows impedance is much smaller [7].

3.5.3 Longitudinal Coupled Bunch Instability

The narrow band impedance of the storage ring, basically the longitudinal and transverse High Order Modes (HOM) excited by beam in the RF cavities, determine the long range wakefields that are a source of the longitudinal and transverse multi-bunch instabilities.
The longitudinal wake fields cause the energy oscillations of the successive bunch leading to the longitudinal coupled bunch instability. In a rigid bunch model, the stored beam consists of M identical macroparticle bunches uniformly filled in M RF buckets of the ring. The beam has M oscillation modes with the phase differences $\Delta\phi = 2\pi m/M$, $(n = 0,1,2...M-1)$ and the frequency pattern of the beam at the single point in the ring contains $(pM+n)$ harmonics of the revolution frequency ω_0 with p an integer ($-\infty$ to ∞). In addition, each bunch performs synchrotron oscillations with the frequency $\omega_s = Q_s\omega_0$ (Q_s is the synchrotron tune). Thus, the observation of the beam at the single point in the ring will detect the signal at the revolution frequency harmonics $(pM+n)\omega_0$ plus the synchrotron frequency ω_s. The spectrum of the beam in macroparticle model is then given by

$$\omega_{np} = (pM + n + Q_s)\omega_0 \tag{3.5.8}$$

If the longitudinal HOM impedance $Z_\parallel(\omega)$ has the components of the same frequencies as the beam signal, strong longitudinal coupled bunch instability is developed. The instability growth is caused by the imaginary part of the complex frequency shift $\Delta\Omega$ that for the $n-th$ beam oscillation mode is given by [2, 6, 8]

$$\Delta\Omega_\parallel^n = iN\frac{\alpha I}{4\pi Q_s(E/e)}\sum_{p=-\infty}^{\infty}\omega_{np}Z_\parallel(\omega_{np})e^{-(\omega_{np}\sigma_\tau)^2} \tag{3.5.9}$$

with I average circulating current, α momentum compaction factor, E/e beam energy (eV), σ_τ bunch length (sec) and N number of cavities. The narrow band impedance $Z_\parallel(\omega)$ of the cavity longitudinal HOM is given by

$$Z_\parallel(\omega) = \sum_{k=1}^{K}\frac{R_\parallel^k}{1+iQ_k\left(\omega_\Gamma^k/\omega - \omega/\omega_\Gamma^k\right)} \tag{3.5.10}$$

where K indicates the highest HOM that is below the cut-off frequency of the vacuum pipe, Q_k and $R_\parallel^k$ are the quality factor and shunt impedance of the excited mode and ω_Γ^k is the resonant frequency.
The coherent oscillations of the bunch with respect to synchronous particles are described by $s(t) = A\exp(i\Delta\Omega_\parallel t)$ and the imaginary part of the complex frequency shift can give rise to an instability when $\mathrm{Im}[\Delta\Omega_\parallel] < 0$, with the growth rate $\alpha_G = 1/\tau = -\mathrm{Im}[\Delta\Omega_\parallel]$. The real part of the $\Delta\Omega_\parallel$ gives the frequency shift. The growth is inconvertible if the growing rate exceeds the damping rate of synchrotron oscillations.
The longitudinal coupled bunch instability for the CANDLE storage ring has been studied for two options of RF cavities: the original ELETTRA cavity [9] and the ELETTRA type cavity adopted for the ANKA [10]. The list of parameters of the longitudinal high order modes of these cavities that have been taken into consideration is given in Table 3.5.3.

Table 3.5.3 Longitudinal HOM's of ELETTRA and ANKA cavities

	ELETTRA			ANKA		
	$f_r\ (MHz)$	$R_{\parallel}\ (M\Omega)$	Q	$f_r\ (MHz)$	$R_{\parallel}\ (M\Omega)$	Q
L1				947.0	1.000	36200
L2	758.2	2.910	37000	1056.	0.048	48400
L3	1048. 5	0.100	34000	1421.6	0.226	44400
L4	1302.	1.340	112000	1511.4	0.193	46000
L5	1328.	0.418	34000	1604.6	0.439	44800
L6	1658.4	0.328	34000	1875.6	0.02	39400
L7	1707.7	0.828	34000	1947.8	0.109	67900
L8	1860.5	0.100	34000	n.m	n.m	n.m
L9	1962.4	0.106	34000	2126.7	0.253	53700
Ll0	2121.5	0.587	34000			
L11	2167.7	0.100	34000			

Fig. 3.5.4 presents the growing rate of longitudinal coupled bunch instabilities versus the relative mode index n for the 282 beam oscillation modes. The two longitudinal modes of ANKA cavity, L4 and L5, drive the instability at the relative oscillation modes of 9 and 76 respectively with the growth rate exceeding the damping rate of synchrotron oscillation. In addition, two longitudinal modes, L2 and L9, are critical so that with low frequency change they can excite the longitudinal coupled bunch instabilities at the beam oscillation modes 41 and 92.

There are nine local maximums on distribution curve for ELETTRA cavity. The growing rates of instabilities are mostly below the synchrotron radiation damping $\alpha_s = 375\sec^{-1}$, except for L6 longitudinal mode that excites the instability at relative oscillation mode of n=115. Although the growing rates of these instabilities are below the synchrotron oscillations damping rate, they have very narrow stable frequency band. For example, the increase of the resonant frequency of ELETTRA cavity longitudinal mode L11 by $0.16\ MHz$ leads to more than fivefold increase of the growing rate of relative mode $n = 122$: from $\alpha_G = 136\sec^{-1}$ up to $\alpha_G = 770\sec^{-1}$ which exceeds the longitudinal radiation dumping rate $\alpha_s = 375\sec^{-1}$ more than twice. Another example is that the decrease of resonant frequency of mode L8, which is responsible for local maximal level $\alpha_G = 13.7\sec^{-1}$ at $n = 260$, by $0.52\ MHz$ changes this value to $2225\sec^{-1}$.

The summary of the most critical longitudinal high order modes for ELETTRA and ANKA type cavities and the corresponding beam oscillation mode numbers as well as the growing rates and the longitudinal frequency shifts of the excited longitudinal coupled instabilities in CANDLE storage ring are presented in Table 3.5.4.

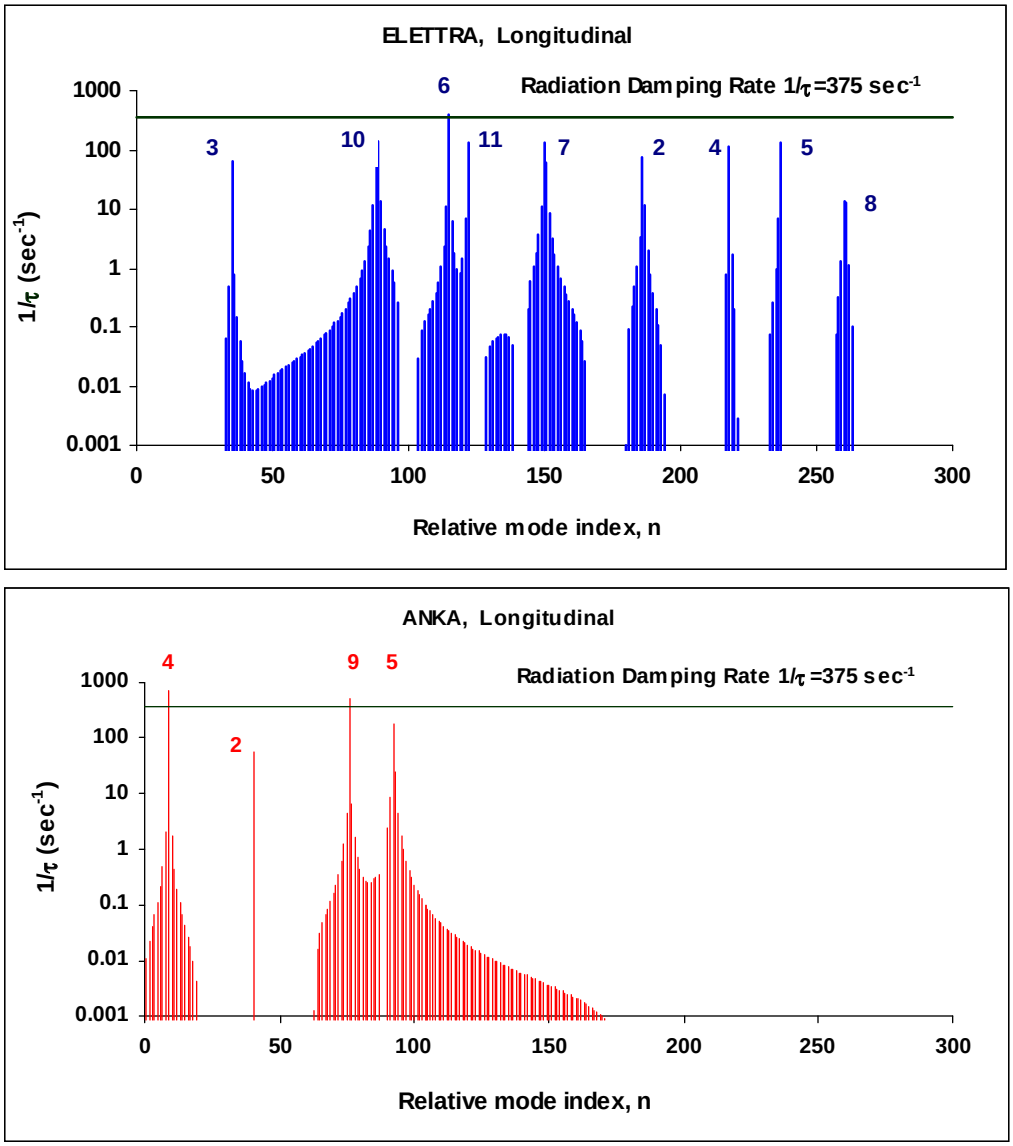

Fig.3.5.4 The growing rate of longitudinal coupled bunch instabilities versus beam oscillation modes in CANDLE for ELETTRA and ANKA type cavities.

Table 3.5.4 Parameters of the ELETTRA and ANKA cavities longitudinal HOMs critical for CANDLE operation .

ELETTRA				ANKA			
N	HOM	$\alpha_G = 1/\tau$	$\Delta\omega_s^n$	n	HOM	$\alpha_G = 1/\tau$	$\Delta\omega_s^n$
35	L3	65.3216	0.00041	9	L4	745.321	-0.0022412
89	L10	141.636	-0.00206	41	L2	55.2361	0.00026077
115	L6	393.557	-0.00227	76	L5	529.535	0.00297564
122	L11	136.14	-0.00083	92	L9	180.557	0.00149131
150	L7	129.217	0.002053				
186	L2	73.7634	0.002020				
218	L4	116.547	0.002230				
237	L5	134.195	-0.00137				
260	L8	13.7375	0.000243				

3.5.4 Transverse Coupled Bunch Instability.

The transverse coupled bunch instabilities are excited by the long range transverse wake fields (transverse HOM) produced by the off-axis beam in the cavities. For the rigid dipole transverse oscillations of the bunches, the mode spectrum lines of the beam in the horizontal (x) and vertical (y) planes are given similar to longitudinal one

$$\omega_p^{x,y} = \left(pM + n + Q_{x,y}\right)\omega_0 \tag{3.5.11}$$

with $Q_{x,y}$ the horizontal and vertical betatron tunes respectively. The complex frequency shift is given by the transverse impedance of the cavity $Z_\perp\left(\omega_p\right)$ as [6]

$$\Delta\Omega_{x,y}^n = -iN\frac{\overline{\beta}_{x,y}\omega_o I}{4\pi\left(E/e\right)}\sum_{p=-\infty}^{\infty} Z_\perp\left(\omega_p\right)e^{-\left(\omega_p\sigma_\tau\right)^2} \tag{3.5.12}$$

with $\overline{\beta}_{x,y}$ the average horizontal and vertical beta-functions and

$$Z_\perp(\omega) = \sum_{k=1}^{K}\frac{\omega_\Gamma^k}{\omega}\frac{R_\perp^k}{1+iQ_k\left(\omega_\Gamma^k/\omega - \omega/\omega_\Gamma^k\right)} \tag{3.5.13}$$

$R_\perp^k$ is the cavity transverse shunt impedance. The transverse oscillations are unstable if the imaginary part of the complex frequency shift is negative. Table 3.5.5 presents the parameters of the transverse HOM of the ELETTRA and ANKA cavities.

Table 3.5.5 Transverse HOMs of ELETTRA and ANKA cavities.

	ELETTRA			**ANKA**		
	$f_r\ (MHz)$	$R_\perp\ (M\Omega/m)$	Q	$f_r\ (MHz)$	$R_\perp\ (M\Omega/m)$	Q
T1	689.0	0.990	45000	743.73	2.6	35500
T2	829.3	11.590	45000	743.94		
T3	1070.8	26.640	40000	746.39	9.0	36400
T4	1137.9	0.270	45000	746.71		
T5	1245.0	3.230	95000	1112.48	10.1	33200
T6	1346.7	1.000	40000	1112.65		
T7	1577.5	1.000	40000	1120.33	0.2	78400
T8	1718.6	1.000	40000	1120.79		
T9	1950.7	1.000	40000	1244.80	2.8	24000
T10	1997.6	1.000	40000	1304.89	0.1	15000
T11	2022.0	1.000	40000	1305.07		
T12	2132.1	1.000	40000	1557.29	0.0	7600
T13				1557.74		
T14				1631.28	1.8	22000
T15				1716.08	1.0	18100
T16				1716.32		

The growing rates of transverse coupled bunch instabilities for horizontal and vertical transverse beam oscillation modes in CANDLE with ELETTRA and ANKA type cavities are presented on Fig. 3.5.5 (horizontal) and Fig. 3.5.6 (vertical).

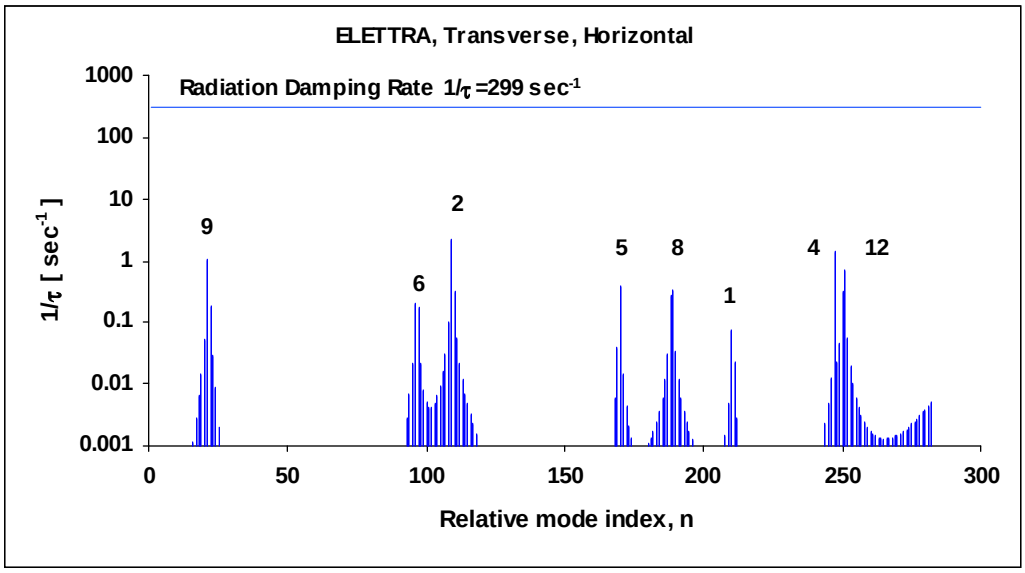

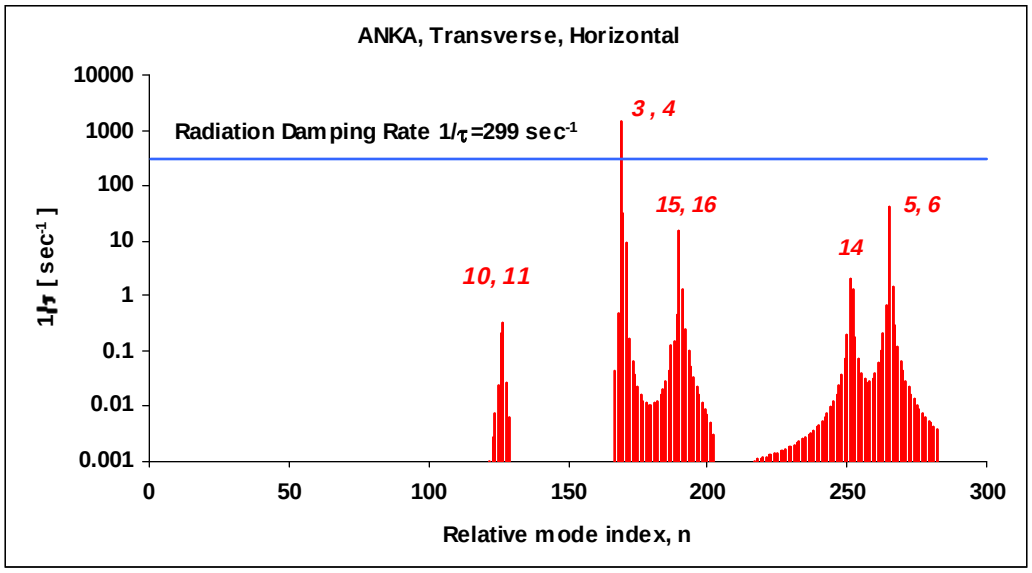

Fig.3.5.5 The transverse coupled bunch instability growing rate versus beam oscillation modes index for ELETTRA and ANKA cavities (horizontal plane).

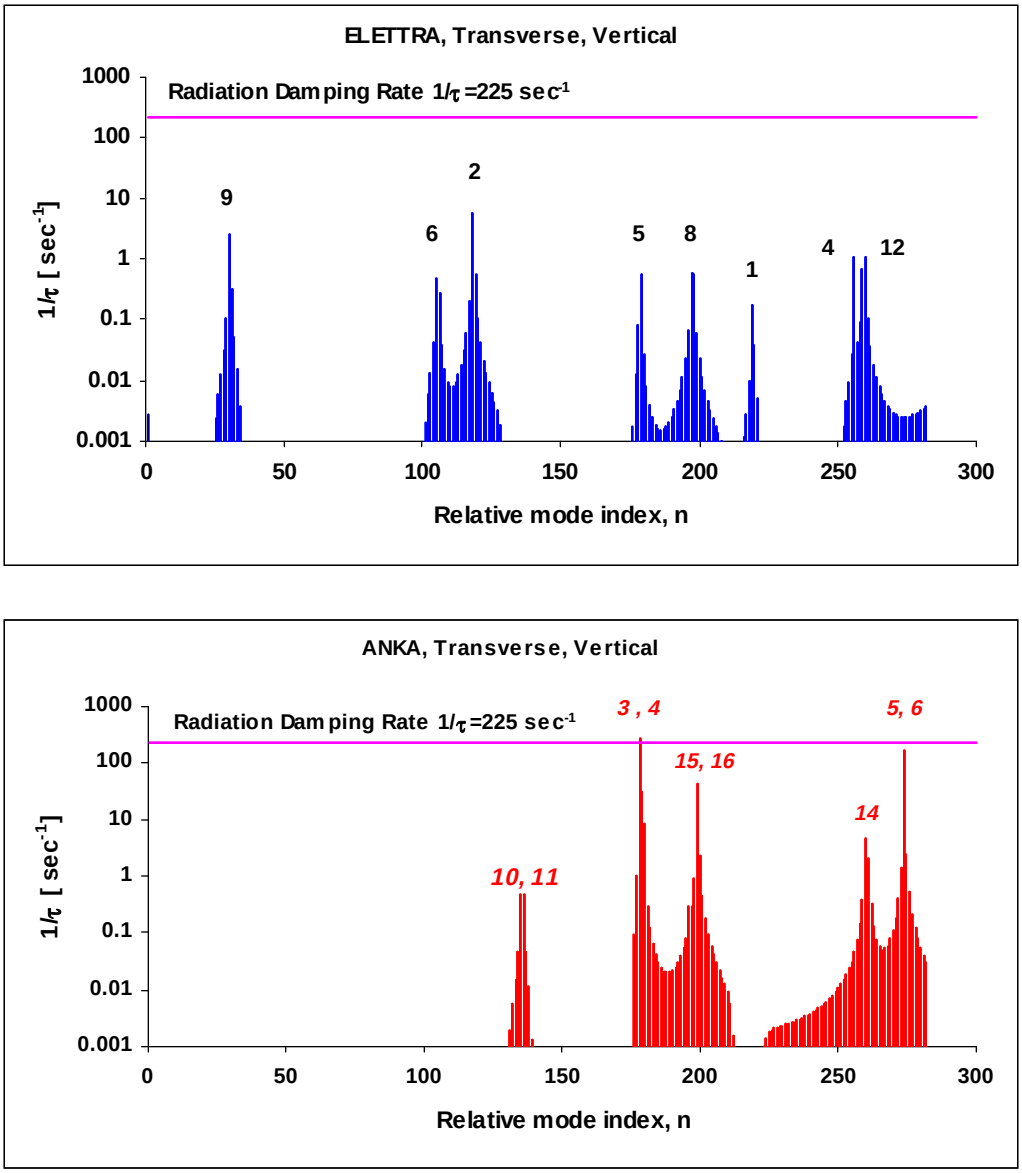

Fig. 3.5.6. The transverse coupled bunch instability growing rate versus beam oscillation modes index for ELETTRA and ANKA cavities (vertical plane).

As it follows from the figures, the modes that excite the coupled bunch instability in the horizontal plane produce unstable transverse oscillations in vertical plane as well. The list of the critical modes for ELETTRA and ANKA cavities for the CANDLE storage ring is presented in Table 3.5.6. The ELETTRA and ANKA cavities have 9 and 5 critical transverse HOM's respectively, that cause unstable coupled bunch oscillations.

As it follows from the comparative analysis of two various ELETTRA type cavities, the existing technologies of the manufacturing of RF cavities lead to individual distinction for each prepared cavity. The cavities will be carefully certified to determine HOMs parameters. Then with the help of methodology presented in this section (see also [11]) the harmful (the growing rate of which is higher than the radiation damping rate) and the critical (the growing rate of which turns higher than the radiation damping rate with the small frequency change) HOMs will be determined. The instability cures will be developed to prevent the longitudinal and transverse beam blow-up in the ring.

Table 3.5.6. The parameters of ELETTRA and ANKA cavities transverse HOMs critical for CANDLE storage ring operation.

Transverse-Horizontal							
ELETTRA				**ANKA**			
N	HOM	$\alpha_G = 1/\tau$	$\Delta\omega_s^n$	n	HOM	$\alpha_G = 1/\tau$	$\Delta\omega_s^n$
21	T9	1.00171	0.0000125		T11	0.114023	-0.0000014
96	T6	0.199391	0.0000057	169	T3	1519.42	0.00104991
109	T2	2.1479	0.0000641		T4	3.16681	-0.0000656
170	T5	0.377919	-0.0000136	190	T15	2.96937	0.00002184
189	T8	0.331033	-0.0000072		T16	11.4877	0.00004225
210	T1	0.075957	0.00000356	251	T14	2.00742	0.0001913
247	T4	1.37758	-0.0000078	265	T5	8.14911	0.000116486
251	T12	0.693805	-0.0000104		T6	33.8066	0.000236431
Transverse-Vertical							
30	T9	2.53003	0.0000275	136	T10	0.314427	-0.0000031
105	T6	0.452543	0.000012		T11	0.186319	-0.0000042
118	T2	5.60516	0.00014	178	T3	263.656	-0.0008406
179	T5	0.532379	-0.000022		T4	4.31118	-0.00010435
198	T8	0.536598	-0.0000126	199	T15	7.16568	0.0000466
219	T1	0.182263	0.0000076		T16	35.7821	0.00010126
256	T4	1.08723	-0.0000096	260	T14	4.58572	0.00005
260	T12	1.09305	-0.000017	274	T5	22.2063	0.0002645
					T6	145.488	0.0006705

References

1. 1-2 GeV Synchrotron Radiation Source, CDR, LBL, Berkeley, 1986.
2. C. Bocchetta, Lifetime and beam quality, CERN 98-04, 1998.
3. A.Hofmann, Single-Beam Collective Phenomena – Longitudinal, Proc. First. Course of Int. School of Particle Accelerators, Erice 1976, CERN 77-13, p/ 139.
4. D.Boussard, Observation of Microwave Longitudinal Instabilities in the CPS, CERN/Lab, II/RF/Int.75-2, 1975.
5. L.J.Lasslett, K.V.Neil and A.M.Sessler, Rev. Sci. Inst., 32, 279, 1961
6. A.Chao, Physics of Collective Beam Instabilities in High Energy Accelerators, J. Wiley and Sons, New York, 1993.
7. SPEAR-3 Design Report, SSRL, Draft Version, Aug., 1999.
8. J.L.Laclare, Bunched Beam Instabilities, Proc., XI-th Conf. High Energy Accelerators, CERN, Geneva, 1980, pp. 526-539.
9. Design Study for the Trieste Syncrotron Light Source, (Sc. Editor S. Tazzari), INFN – Laboratori Nazionali di Frascati, LFN-87/6(R), 1987.
10. P.Craievich, A.Fabris, C.Pasotti, M.Svandrlik, HOM Characterisation of the ANKA RF Cavities for Coupled Bunch Instability Calculations, PAC-99, pp. 1123-1125, New York, 1999.
11. Y. Martirosyan, M. Ivanyan, V. Tsakanov, Beam Current Limitations Study for CANDLE Light Source, EPAC-2002, Jun. 2002, Paris (to be published).